ISSN 2075-1133, Inorganic Materials: Applied Research, 2021, Vol. 12, No. 5, pp. 1400–1408. © Pleiades Publishing, Ltd., 2021.
Russian Text © The Author(s), 2021, published in Perspektivnye Materialy, 2021, No. 6, pp. 60–72.

NEW TECHNOLOGIES OF PRODUCTION AND PROCESSING OF MATERIALS

Kinetics of Low-Temperature Aluminothermic Reduction of Iron Tantalate

R. I. Gulyaeva[a, *], **A. M. Klyushnikov**[a, **], **S. A. Petrova**[a, ***], **and L. Yu. Udoeva**[a, ****]
[a] *Institute of Metallurgy, Ural Branch, Russian Academy of Sciences, Yekaterinburg, 620016 Russia*
**e-mail: gulroza@mail.ru*
***e-mail: amk8@mail.ru*
****e-mail: danaus@mail.ru*
*****e-mail: lyuud@yandex.ru*

Received November 10, 2020; revised November 25, 2020; accepted November 26, 2020

Abstract—The kinetics of low-temperature (900–1180°C) reduction of iron tantalate (98.2 wt % $FeTa_2O_6$, 1.8 wt % Ta_2O_5, and particle size <0.1 mm) with an excess of aluminum (particle size <0.14 mm) and Al : $FeTa_2O_6$ molar ratio equal to 6 is studied. The differential scanning calorimetry and X-ray phase analysis data show that the reduction process terminates approximately at 1180°C to form TaFeAl, $TaAl_3$, and $Ta_{17}Al_{12}$ metal products. The thermokinetic calculations (Ozawa–Flynn–Wall and nonlinear regression methods) indicate that the formal mechanism of the process is as a Bna → CnC scheme, which includes two successive stages controlled by the reactions activated autocatalytically. The kinetic parameters of the stages are as follows: (1) $E_1 = 429$ kJ mol^{-1} and $A_1 = 10^{15.3}$ s^{-1} and (2) $E_2 = 176$ kJ mol^{-1} and $A_2 = 10^{3.9}$ s^{-1} (where E_j is the activation energy and A_j is the pre-exponential factor). The prediction within the Bna → CnC model indicates that the reaction mixture containing ≥98 mol % of a formal final reduction product may be obtained within 1040–1120°C over a period of 1.5–5 min. The proposed model can be used to develop scientific foundations and to substantiate technological modes of obtaining tantalum alloys from mineral and technogenic raw materials.

Keywords: iron tantalate, reduction, aluminothermy, thermodynamics, kinetics

DOI: 10.1134/S2075113321050130

INTRODUCTION

One of the sources of tantalum are concentrates containing minerals of the tantalum niobate group, which are as isomorphic complex oxides with a general formula (Fe,Mn)(Nb,Ta)$_2$O$_6$ [1]. Pure tantalum can be obtained from such concentrates via acid leaching to transfer tantalum and niobium into solution, the liquid extraction of tantalum, the aluminothermal reduction of Ta_2O_5 with iron or manganese alloy additions (as metals or oxides), heating in vacuum, and electron beam melting of Ta–Al–Fe or Ta–Mn–Fe alloys [2]. Alloying additives and excess aluminum during the reduction of Ta_2O_5 are necessary to decrease the melting temperatures of alloy and slag and their effective separation in the liquid phase [3]. Meanwhile, the elemental composition of tantalum niobates makes it possible to obtain tantalum alloys via direct aluminothermic reduction of tantalum-containing concentrates.

The development of the scientific foundations of such a technology requires data on the interaction between aluminum and tantalum niobates of various compositions, including that enriched in tantalum and iron with an extreme formula of $FeTa_2O_6$. This compound is dimorphic and can exist as ferrotantalite and ferrotapiolite minerals crystallized in the rhombic and tetragonal modifications, respectively [4]. There are no data on the thermodynamics and the kinetics of its direct aluminothermic reduction in the literature. The results of study of interaction of aluminum with simple tantalum, niobium, and chromium oxides and pyrochlore concentrates [5–7], as well as the chemistry of reduction of synthetic manganese tantalate and iron niobate [8, 9], may be used only as initial data to understand the aluminothermic reduction of iron tantalate. High temperature of aluminothermic processes determines their intense dynamics. The completeness and the rate of interaction between liquid aluminum and solid oxides, however, have a significant influence on the reduction parameters as a whole [6].

The aim of this work is to study the kinetics of low-temperature interaction between iron tantalate and an excess of aluminum.

EXPERIMENTAL

An iron tantalate sample was synthesized via the solid-phase sintering of a mixture of iron(II) oxide

(99.2 wt % FeO) and tantalum(V) oxide (99.9 wt % β-Ta_2O_5). The samples of powdered (particle size <0.1 mm) chemically pure iron(III) oxide (99 wt % Fe_2O_3) and carbonyl iron (99.96 wt % Fe) used in a stoichiometric ratio were mixed, briquetted on a hydraulic press (100 MPa), and placed into a quartz tube, which was then evacuated to a residual pressure of 10^{-4} atm and kept in an electric muffle furnace for 360 h at 700°C to obtain iron(II) oxide. The resulting product was cooled in an oven and ground in an agate mortar to a particle size of <0.1 mm. The weighed amount of a grade B metallurgical tantalum powder (99.5 wt % Ta; particle size <0.1 mm) was placed into an alundum boat and kept in an electric muffle furnace with access air for 4 h at 1100°C to synthesize tantalum(V) oxide. The resulting product was cooled in air, ground in an agate mortar to a particle size of <0.1 mm, and heated repeatedly under similar conditions. The samples of iron(II) and tantalum(V) oxides used in a stoichiometric ratio were mixed, briquetted in a hydraulic press (100 MPa), and kept in an alundum boat of a tubular electric furnace for 12 h at 1200°C, in the working chamber of which helium (99.995 vol % He) was supplied continuously at a flow rate of 30 cm^3 min^{-1}. The resulting product was cooled in an oven and ground in an agate mortar to a particle size of <0.1 mm. The temperature was measured on a chromel-alumel thermocouple with an error of ±10°C in all cases.

The PA4 aluminum powder with a particle size of <0.14 mm containing ≥98, ≤0.35, ≤0.40, ≤0.02, and ≤0.2 wt % of Al, Fe, Si, Cu, and H_2O, respectively, was used as a reduction agent.

The aluminum and iron tantalate samples used in an Al : $FeTa_2O_6$ molar ratio equal to 6 were thoroughly mixed and compacted in an alundum crucible. The elemental and phase composition of the mixtures was calculated by means of HSC Chemistry 6.12 software [10].

The aluminothermic reduction of iron tantalate was performed with combined thermogravimetry (TG) and differential scanning calorimetry (DSC) on a NETZSCH STA 449 C Jupiter thermal analyzer. The samples (25.2–30.2 mg) of the mixtures were placed into an alundum crucible with a lid having a calibrated hole, heated from 30 to 1180°C, and then cooled from 1180 to 500°C at rates of 10, 15, and 20°C min^{-1} in an argon flow (99.995 vol % Ar) at 50 cm^3 min^{-1}. A calcined alundum crucible served as the reference material. The measurement errors for the mass, temperature, and heat were ±0.01 mg, ±3°C, and ±5%, respectively. The correction parameters were assessed from the enthalpy of melting of chemically pure indium (99.99 wt % In) with NETZSCH Thermokinetics 3.0 software [11].

The iron tantalate samples and its reduction products were studied with X-ray phase analysis (XRD) on a Bruker D8 ADVANCE spectrometer. The data were recorded in the range of 5°–130° and 5°–90° (2θ) for the starting tantalate and its interaction products with aluminum, respectively, with a step of 0.021° (2θ) and exposure of 493 s. The acquisition parameters were as follows: Cu K_α radiation ($\lambda = 0.154051$ nm), the voltage of 34 kV, the current on a tube of 40 mA, and VÅNTEC–1 position-sensitive detector. A β filter and Bragg–Brentano geometry were used. The ICDD PDF-4 database was used to identify the phases [12]. The crystal structure of the samples was assessed with application of DIFFRAC.EVA software [13]. The unit cell parameters of the phases were calculated by the least squares method using the Celref program [14]. The quantitative phase analysis and the refinement of structural parameters of the phases were performed by the Rietveld method [15] using the TOPAS program [16].

The aluminothermic reduction of iron tantalate was simulated thermodynamically via minimization of the standard Gibbs energy (ΔG_T) of phases within 500–3000°C and at Al : $FeTa_2O_6$ molar ratios from 1 to 6 using HSC Chemistry 6.12 software [10]. The standard enthalpy of formation (ΔH_{f298} in kJ mol^{-1}), the entropy of formation (ΔS_{f298} in J mol^{-1} K^{-1}), and the relationships between the coefficients of isobaric heat capacity ($C_{p,T} = A + B \times 10^{-3}\ T + C \times 10^{5} T^{-2} + D \times 10^{-6} T^{2}$, in J mol^{-1} K^{-1}) and the absolute temperature (T in K) for $FeTa_2O_6$, Ta_2Al, and $TaAl_3$ not found in the program database were taken from published sources or were calculated according to known methods [17–21] (Table 1). The gaseous N_2 and some condensed compounds (Al_2O_3, $FeTa_2O_6$, FeO, Fe_2O_3, Fe_3O_4, Ta_2O_5, $FeAlO_4$, Al, Fe, Ta, Fe_2Ta, Ta_2Al, and $TaAl_3$) were considered.

The DSC data for heating a mixture of reagents at the Al : $FeTa_2O_6$ ratio equal to 6 were processed using the following kinetic equations to assess the effective activation energy, the pre-exponential factor, and the number of formal stages of the aluminothermic reduction reaction of iron tantalate [22–24]:

$$\frac{d\alpha}{dt} = k(T)f(\alpha) = A\exp\left(-\frac{E}{R(T_{in} + \beta t)}\right)f(\alpha), \qquad (1)$$

$$\alpha = \frac{\int_{T_{\mathrm{in}}}^{T}\left(\frac{dH}{dT}\right)dT}{\int_{T_{\mathrm{in}}}^{T_f}\left(\frac{dH}{dT}\right)dT}, \qquad (2)$$

where α is the degree of conversion of the starting reagent into a product; t the time (s); dH the infinitesimal change in enthalpy of reaction (J g^{-1}); $d\alpha/dt$ the conversion rate (s^{-1}); $k(T)$ is the rate constant of a reaction (s^{-1}); T_{in}, T, and T_f are the absolute temperatures of a sample at the initial, current, and final moments of the reaction, respectively (K); A is the pre-exponential factor (s^{-1}); E is the effective activation energy of the reaction (J mol^{-1}); R the universal gas constant (J mol^{-1} K^{-1}); $f(\alpha)$ the kinetic model of

Table 1. Thermodynamic properties of $FeTa_2O_6$, Ta_2Al, and $TaAl_3$ in the temperature range from T_1 to T_2

Phase	Enthalpy, $\Delta H_{f,298}$, kJ mol^{-1}	Enthropy, $\Delta S_{f,298}$, J mol^{-1} K^{-1}	Coefficients of dependence of isobaric heat capacity				$T_1 - T_2$, K
			A	B	C	D	
$FeTa_2O_6$	−2365.6	200.7	197.40	47.83	−31.80	−19.72	323–1203
Ta_2Al	−70.62	111.3	87.67	−22.54	−7.2	0	298–933
$TaAl_3$	−122.36	126.34	126.26	−62.97	−13.95	0	298–933

Table 2. Properties of phases identified in iron tantalate sample

Phase	Space group	Unit cell parameters				Amount, wt %	PDF [12]
		a, Å	b, Å	c, Å	V, Å^3		
$FeTa_2O_6$	$P4_2/mnm$	4.7565(1)	–	9.1992(1)	208.13(1)	98.2	04–007–9309
Ta_2O_5	$Pmmm$	6.193(2)	3.663(1)	3.890(1)	88.26(4)	1.8	04–013–9608

the reaction; and β the rate of temperature change (K s^{-1}) ($\beta = dT/dt$).

The model dependent kinetic analysis (implying that the process mechanism is one-stage) was performed using the following expression, which is Eq. (1) transformed within the framework of the Ozawa–Flynn–Wall formalism [25–27]:

$$\ln\beta_i = \text{const} - 1.052\frac{E_\alpha}{RT_{\alpha,i}}. \quad (3)$$

The relationship between $\ln\beta_i$ and $1/T_{\alpha,i}$ was approximated linearly, the E_α value was assessed from the slope of isoconversion line, and A_α was found from the point of its intersection with the y axis (assuming that the reaction is first-order) for a series of temperature programs (β_i = 10, 15, and 20°C min^{-1}) and a number of α values. The subscripts α and i indicate that the corresponding values are taken at fixed α and β values. The number (j) of elementary stages is found for the multistage process from the form of the relationship between E_α and α. The kinetic parameters (A_j and E_j) of the stages were refined via nonlinear regression by selecting an acceptable standard reaction model $f_j(\alpha_j)$ [22]. The data obtained were used to give the kinetic equations of elementary stages as analytical expressions [23, 28]:

$$\frac{d\alpha_j}{dt} = A_j \exp\left(-\frac{E_j}{RT}\right) f_j(\alpha_j), \quad (4)$$

where α_j is the degree of conversion of the starting reagent of the jth stage into its final product. The degree of conversion (α_Σ) of the starting formal reagent of the total reaction into its formal products was found from the following equation [23]:

$$\alpha_\Sigma = \sum_j w_j \alpha_j, \quad (5)$$

where w_j is the contribution of the thermal effect of the jth stage to the total thermal effect of the reaction. The process model selected was used to predict the kinetics of reduction of iron tantalate in the isothermal regime. NETZSCH Thermokinetics 3.0 software was used for the calculations [11].

RESULTS AND DISCUSSION

The diffraction pattern of the iron tantalate sample synthesized (Fig. 1) shows the reflections of ferrotapiolite with a tetragonal structure (04–007–9309 [12]) and tantalum(V) oxide with an orthorhombic structure (04–013–9608 [12]). Table 2 shows the properties of the phases. The amount of Ta_2O_5 impurity in iron tantalate is no more than 1.8 wt %.

The process was simulated thermodynamically to select the optimal reduction regime. Figure 2 indicates that the reduced tantalum and iron can exist both in the elemental form and as Fe_2Ta, Ta_2Al, and $TaAl_3$ intermetallic compounds in the composition of interaction products. The metal phase mainly consists of tantalum compounds with iron and aluminum at low temperatures, but it has a high amount of tantalum with an increase in temperature. An analysis of the relationship between the change in composition of the reaction products and the amount of a reduction agent makes it possible to deduce the following transformation sequence of tantalum-containing phases in the system:

$$\begin{gathered} FeTa_2O_6 \rightarrow Fe \rightarrow Ta_2O_5 \rightarrow Fe_2Ta + Ta \\ \rightarrow Ta + Fe_2Ta + Ta_2Al + TaAl_3. \end{gathered} \quad (6)$$

Complete reduction of tantalum and iron from oxides at 1200°C can be expected when the Al : $FeTa_2O_6$ ratio is no less than 4 and 1, respectively. Considering that the melting point of metal reduction products can be decreased owing to the formation of

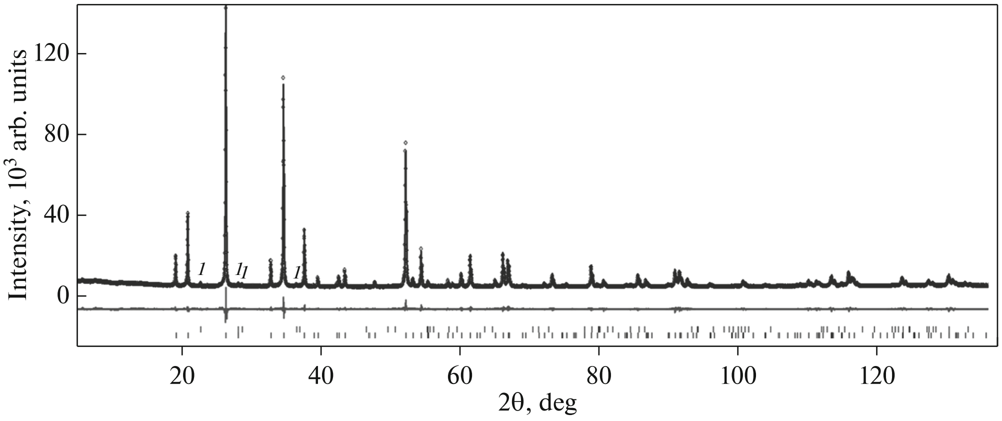

Fig. 1. XRD pattern of iron tantalate sample and full-profile analysis data: points and lines on XRD pattern show experimental and calculated curves, respectively; the horizontal line below is the difference curve; vertical strokes are Bragg reflections allowed for each phase; and (*1*) lines of Ta_2O_5. Reliability factors: expected factor $R_{exp} = 2.17$, profile-weighted factor $R_{wp} = 2.87$, profile factor $R_p = 2.20$, and goodness of fit GoF = 1.32.

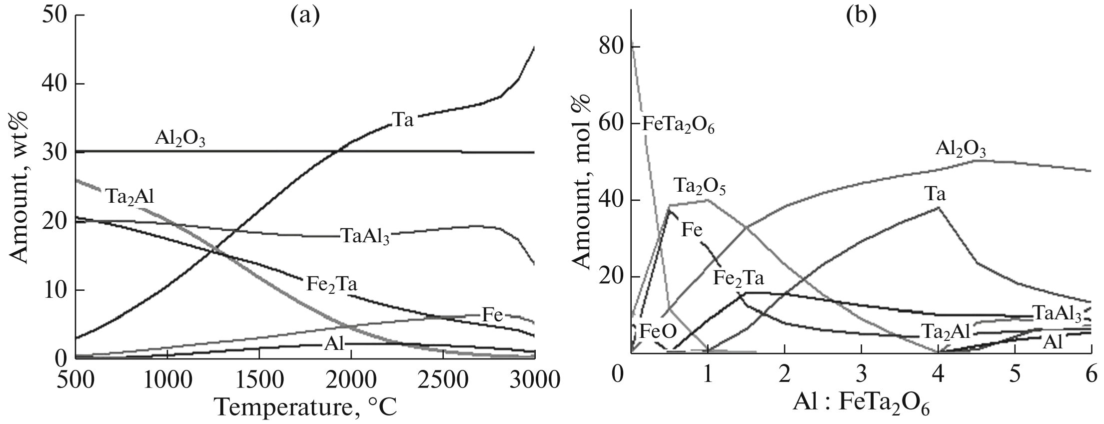

Fig. 2. Changes in equilibrium composition of reaction mixture during aluminothermic reduction of $FeTa_2O_6$ depending on (a) temperature for molar ratio Al : $FeTa_2O_6$ = 6 and (b) molar ratio Al : $FeTa_2O_6$ at 1200°C.

intermetallic phases, an excess of a reduction agent corresponding to the Al : $FeTa_2O_6$ molar ratio equal to 6 was used in the experiments. The composition of a mixture of iron tantalate with aluminum used in the experiments was calculated from XRD data (Table 3).

When a mixture of iron tantalate with aluminum is heated from 30 to 1180°C ($\beta = 10°C\ min^{-1}$), some effects are observed on the DSC curve (Fig. 3). The endothermic peak with start/maximum at 647/661°C is assigned to the melting of aluminum [29]. Two exothermic peaks with start/maximum temperatures of 891/899 and 987/1032°C and heats of 7 and 415 J g^{-1} are probably due to the reduction reactions of tantalum oxide and iron tantalate, respectively. The DSC data within 900–1117°C were used for the subsequent kinetic analysis in this regard. The endothermic peak with start/maximum at 1115/1130°C indicates the melting of one of the low-melting reduction products: the Fe–Al–Ta eutectic [29]. The exothermic effect with start/maximum temperatures at 1125/1123°C appearing on the DSC curve after cooling of the reaction mixture from 1180 to 500°C is due to the crystal-

Table 3. Calculated composition of mixture of aluminum with iron tantalate used in experiments

Elemental composition, wt %					Phase composition, wt %.			
Fe	Ta	Al	O	Other	$FeTa_2O_6$	Ta_2O_5	Al	Other
8.1	53.7	23.5	14.2	0.5	74.6	1.4	23.5	0.5

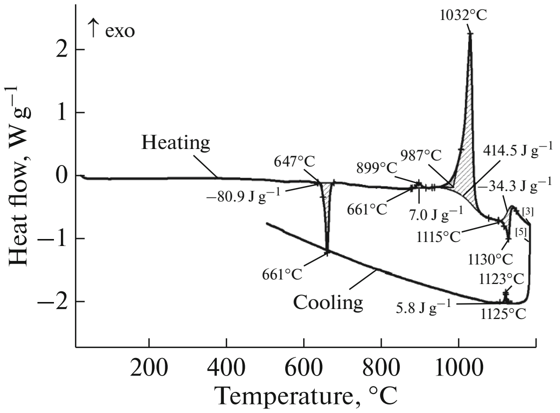

Fig. 3. DSC curve of mixture of iron tantalate and aluminum during heating from 30 to 1180°C and cooling to 500°C ($\beta = 10°C\ min^{-1}$) in argon flow.

lization of this eutectic. The shape of a curve during cooling indicates that there is no aluminum unreacted in the reduction products. The weight of the sample changed by 0.30% during its heating to 1180°C, which is due to an insignificant amount of oxygen in the argon used.

The results of full-profile analysis of diffraction patterns of the products obtained after heating from 30 to 1180°C and cooling of a mixture of iron tantalate with aluminum (Fig. 4 and Table 4) confirm the thermodynamic simulation data that the metals can be reduced almost completely from iron tantalate at low temperatures (about 1200°C). Insignificant amounts of starting reagents unreacted (≤0.4, 0.6–1.2, and 1.8–2.9 wt % of Al, $FeTa_2O_6$, and Ta_2O_5, respectively) and intermediate oxides (1.5–3.1 and 2.1–2.2 wt % of $Al_{0.5}Ta_{0.5}O_2$ and $Fe_{0.5}Ta_{0.5}O_2$, respectively) confirm these observations. The amount of metal reduction products (TaFeAl, $TaAl_3$, and $Ta_{17}Al_{12}$) is 60.0–66.7 wt %. It should be noted that the composition of the products is changed insignificantly depending on a heating rate (Fig. 5). Indeed, the amount of TaFeAl, $Ta_{17}Al_{12}$, and Al_2O_3 increases with its decrease, whereas that of $TaAl_3$ decreases. This indicates that $TaAl_3$, from which the TaFeAl and $Ta_{17}Al_{12}$ intermetallic compounds are additionally formed during slower or more prolonged heating, is primarily formed.

The following chemical processes are assumed on the basis of the data obtained:

$$FeTa_2O_6 + 6Al = Fe + 2TaAl_3 + 2Al_2O_3, \qquad (7)$$

$$FeTa_2O_6 + 14/3\,Al = 1.5Ta + 0.5Fe + Fe_{0.5}Ta_{0.5}O_2 + 4/3\,Al_2O_3, \qquad (8)$$

$$FeTa_2O_6 + 2/3\,Al = Fe + Ta_2O_5 + 1/3\,Al_2O_3, \qquad (9)$$

$$Fe_{0.5}Ta_{0.5}O_2 + 4/3\,Al = 0.5Fe + 0.5Ta + 2/3\,Al_2O_3, \qquad (10)$$

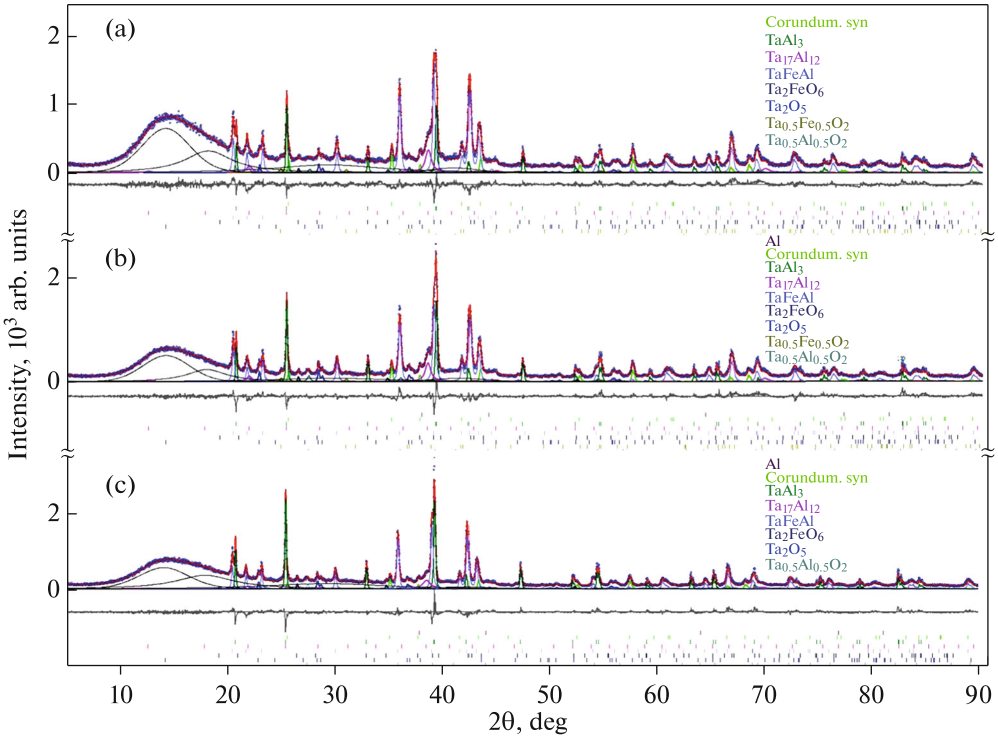

Fig. 4. XRD patterns of products of heating from 30 to 1180°C and cooling in argon flow of mixture of iron tantalate with aluminum: (a) $\beta = 10$, (b) $\beta = 15$, and (c) $\beta = 20°C\ min^{-1}$.

Table 4. Composition and structural properties of phases identified in heating products from 30 to 1180°C and cooling (β = 10, 15, and 20°C min^{-1}) in argon flow of mixture of iron tantalate with aluminum

Phase	Space group	Unit cell parameters				Amount, wt %	PDF [12]
		a, Å	*b*, Å	*c*, Å	*V*, $Å^3$		
Al	*Fm*-3*m*	4.095	–	–	68.69	0.0–0.4	04–012–7848
Al_2O_3	*R*-3*c*	4.757	–	12.995	254.64	33.2–37.5	04–015–8608
$TaAl_3$	*I*4/*mmm*	3.840	–	8.545	126.03	11.1–21.6	04–001–3363
$Ta_{17}Al_{12}$	*I*-43*m*	9.904	–	–	971.51	5.9–7.8	04–003–2132
TaFeAl	*P*63/*mmc*	4.998	–	8.156	176.42	31.9–37.3	04–005–0134
$FeTa_2O_6$	*P*4$_2$/*mnm*	4.754	–	9.207	208.11	0.6–1.2	04–007–9309
Ta_2O_5	*Pmmm*	6.217	3.646	3.877	87.87	1.8–2.9	04–013–9608
$Al_{0,5}Ta_{0,5}O_2$	*P*42/*mnm*	4.591	–	2.970	62.61	1.5–3.1	04–002–2521
$Fe_{0,5}Ta_{0,5}O_2$	*Pbcn*	4.634	5.621	4.904	127.74	2.1–2.2	04–005–8833

$$17FeTa_2O_6 + 97Al = Ta_{17}Al_{12} + 17FeTaAl + 34Al_2O_3, \quad (11)$$

$$TaAl_3 + 3Fe + 2Ta = 3FeTaAl, \quad (12)$$

$$Ta_2O_5 + Al_2O_3 = 4Al_{0.5}Ta_{0,5}O_2, \quad (13)$$

$$7.727TaAl_3 + 4.636Ta_2O_5 + 4.273Al = Ta_{17}Al_{12} + 7.727Al_2O_3. \quad (14)$$

The kinetic parameters of aluminothermic reduction of iron tantalate in the temperature range of 900–1117°C obtained within the Ozawa–Flynn–Wall analysis (Figs. 6 and 7) indicate two controlling stages of the process. The kinetic parameters of the stages vary within the following limits (Table 5): α = 0.02–0.4, E = 204–245 kJ mol^{-1}, and log$A$ = 4.56–6.78 s^{-1} for the first one and α = 0.4–0.98, E = 164–214 kJ mol^{-1}, and log$A$ = 3.97–5.77 s^{-1} for the second one.

The results of nonlinear regression analysis of experimental data (Fig. 8 and Table 6) indicate that the kinetics of low-temperature reduction stage can be described with a high reliability level and adequacy by a sequence of two controlling stages:

$$A \xrightarrow{k_1} B \xrightarrow{k_2} C. \quad (15)$$

The first stage is controlled by an autocatalytic reaction described with the extended Prout–Tompkins equation (Bna) [11] and is characterized by the following parameters: E_1 = 429 kJ mol^{-1}, $A_1 = 10^{15.3}$ s^{-1}, $f_1(\alpha_1) = (1 - \alpha_1)^{0.73}\alpha_1^{0.24}$, and $w_1 = 0.33$.

The second stage is controlled by the *n*th order autocatalytic reaction (CnC) [11] and its kinetic parameters are as follows: E_2 = 176 kJ mol^{-1}, $A_2 = 10^{3.9}$ s^{-1}, $f_2(\alpha_2) = (1-\alpha_2)^{0.63}(1 + 29.51\alpha_2)$, and $w_2 = 0.67$; the resulting products are a catalyst.

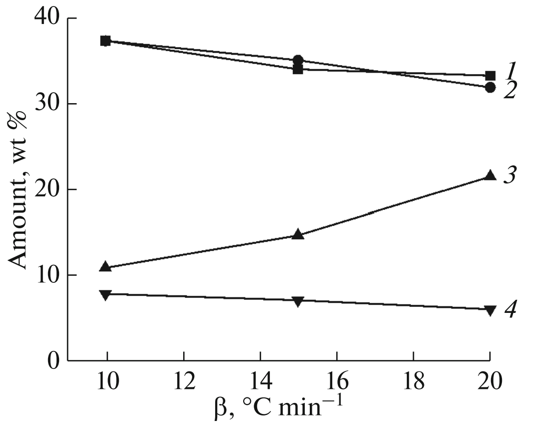

Fig. 5. Change in amount of phases in low-temperature aluminothermic reduction products of iron tantalate depending on heating rate: (*1*) Al_2O_3, (*2*) TaFeAl, (*3*) $TaAl_3$, and (*4*) $Ta_{17}Al_{12}$.

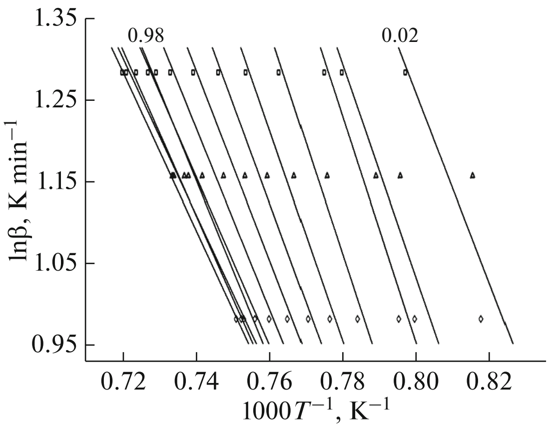

Fig. 6. Ozawa–Flynn–Wall plot constructed from DSC heating data (900–1117°C and β = 10, 15, and 20°C min^{-1}) in argon flow of mixture of iron tantalate with aluminum.

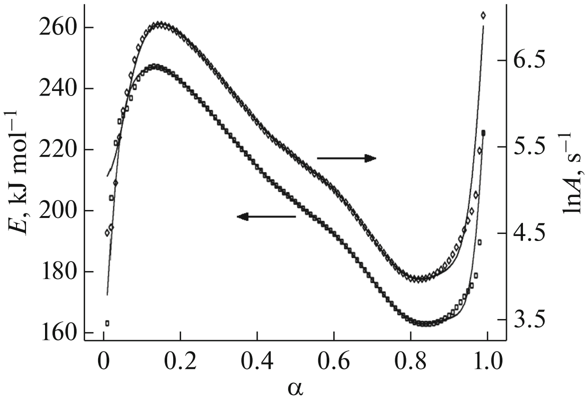

Fig. 7. Changes in kinetic parameters of low-temperature aluminothermic reduction of iron tantalate depending on degree of conversion (Ozawa–Flynn–Wall analysis results).

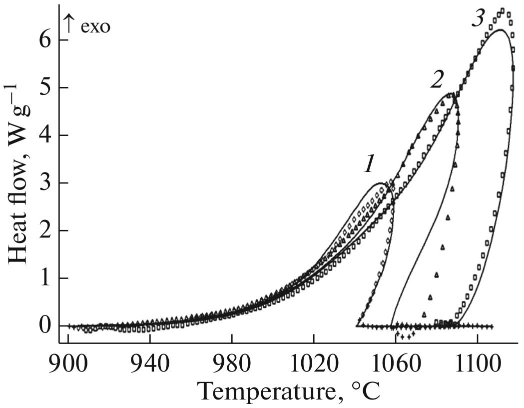

Fig. 8. (points) Experimental and (lines) their approximating calculated DSC heating curves in argon flow of mixture of iron tantalate with aluminum at various β: (*1*) 10, (*2*) 15, and (*3*) 20°C min^{-1}.

The equations describing the kinetics of aluminothermic reduction of iron tantalate (Al : $FeTa_2O_6$ = 6) at 900–1117°C in a two-stage approximation (Bna → CnC) can be represented in analytical form as follows:

$$\frac{d\alpha_1}{dt} = 10^{15.3}(1-\alpha_1)^{0.73}\alpha_1^{0.24}\exp\left(-\frac{429\,000}{RT}\right), \quad (16)$$

$$\frac{d\alpha_2}{dt} = 10^{3.9}(1-\alpha_2)^{0.63} \times (1+29.51\alpha_2)\exp\left(-\frac{176\,000}{RT}\right), \quad (17)$$

$$\alpha_\Sigma = 0.33\alpha_1 + 0.67\alpha_2. \quad (18)$$

The simulation results of isothermal kinetics of the reduction of iron tantalate within the Bna → CnC model (Fig. 9) indicate that the interactions are intense. A reaction mixture containing ≥98 mol % of a formal final reduction product can be obtained during the isothermal holding within 1040–1120°C for 1.5–5 min.

The aluminothermic reduction process of iron tantalate leads to active heat release, and the interaction reaction between liquid aluminum and solid oxide spreads throughout the system after local initiation. The melting point of $FeTa_2O_6$ is 1614°C [17], and the $FeO–Ta_2O_5$ and $Al_2O_3–Ta_2O_5$ intermediate oxides also remain in the solid state under experimental conditions [30, 31]. The mechanism of reactions in the

Table 5. Kinetic parameters of low-temperature aluminothermic reduction of iron tantalate calculated within Ozawa–Flynn-Wall theory

Degree of conversion of starting reagent into product, α	Effective activation energy of reaction, E, kJ mol^{-1}	Pre-exponential factor, log$A$, s^{-1}
0.02	204 ± 116	4.56
0.05	231 ± 106	5.90
0.10	245 ± 80	6.74
0.20	243 ± 55	6.78
0.30	229 ± 42	6.31
0.40	214 ± 33	5.77
0.50	203 ± 30	5.36
0.60	192 ± 27	4.99
0.70	178 ± 19	4.44
0.80	164 ± 16	3.97
0.90	166 ± 4	4.17
0.95	174 ± 13	4.63
0.98	190 ± 20	5.44

Table 6. Kinetic parameters of low-temperature aluminothermic reduction of iron tantalate calculated within two-stage (Bna → CnC) model of process

Parameter	Formal stages of process	
	first stage	second stage
Reaction model	Extended Prout–Tompkins equation (Bna)	Reaction of *n*th order with autocatalysis (CnC)
$f_j(\alpha_j)$	$(1-\alpha_1)^n\alpha_1^m$	$(1-\alpha_2)^n\ (1+K_{cat}\alpha_2)$
E_j, kJ mol^{-1}	429 ± 21	176 ± 4
$\log A_j$, s^{-1}	15.3 ± 0.8	3.9 ± 0.2
$\log K_{cat}$	–	1.47 ± 0.09
n_j	0.73 ± 0.06	0.63 ± 0.03
m_j	0.24 ± 0.06	–
w_j	0.33	0.67

Statistical characteristics of the calculation: $r = 0.994$, $d = 0.023$, $F_{exp} = 1$, $F_{crit}(0.95) = 1.12$, $t_{crit}(0.95) = 1.954$ (*r* is the correlation coefficient, *d* is the Durbin–Watson criterion, F_{exp} and $F_{crit}(0.95)$ are, respectively, the experimental and critical values of the Fisher criterion with a confidence probability of 95%, $t_{crit}(0.95)$ is the critical value of the Student criterion with a confidence probability of 95%.

liquid and solid phases is complex and includes the reaction diffusion processes. Since the starting particles of reagents are sufficiently dispersed, the resulting solid products ($Fe_{0.5}Ta_{0.5}O_2$, $Al_{0.5}Ta_{0.5}O_2$, and Al_2O_3) apparently do not prevent the diffusion of liquid aluminum to the reaction surface. As a result, the process is controlled by the reactions activated autocatalytically, with one or more metal products as catalysts.

The proposed model of aluminothermic reduction of iron tantalate reflects the fundamental kinetic laws and macromechanism of the process despite the fact that it is calculated for a certain reagent mode (Al : $FeTa_2O_6$ = 6) and component size (<0.14 mm). It can be useful to develop and to substantiate the technological regimes for obtaining alloys from tantalum-containing raw materials.

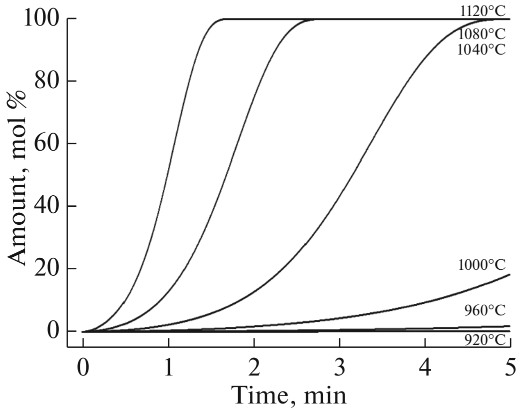

Fig. 9. Predicted effect of temperature and duration of isothermal holding on amount of formal resulting product of low-temperature aluminothermic reduction of iron tantalate in reaction mixture for two-stage (Bna → CnC) model of process.

CONCLUSIONS

The reduction of iron tantalate (98.2 and 1.8 wt % of $FeTa_2O_6$ and Ta_2O_5, respectively; particle size <0.1 mm) with an excess of aluminum (particle size <0.14 mm) at the Al : $FeTa_2O_6$ molar ratio equal to 6 is almost completed up to 1180°C. The metal interaction products are TaFeAl, $TaAl_3$, and $Ta_{17}Al_{12}$. A low amount of $Al_{0.5}Ta_{0.5}O_2$ and $Fe_{0.5}Ta_{0.5}O_2$ intermediate oxides can be formed.

The formal mechanism of the process can be represented by a scheme that includes two successive limitation stages. The first stage is controlled by an autocatalytic reaction described by the extended Prout–Tompkins equation (Bna) and has the following parameters: $E_1 = 429$ kJ mol^{-1}, $A_1 = 10^{15.3}$ s^{-1}, $f_1(\alpha_1) = (1-\alpha_1)^{0.73}\alpha_1^{0.24}$, and $w_1 = 0.33$. The second one is controlled by the *n*th order reaction with autocatalysis (CnC): $E_2 = 176$ kJ mol^{-1}, $A_2 = 10^{3.9}$ s^{-1}, $f_2(\alpha_2) = (1 - \alpha_2)^{0.63}(1 + 29.51\alpha_2)$, and $w_2 = 0.67$; the resulting metal products are catalysts. A reaction mixture containing ≥98 mol % of a formal final reduction product can be obtained with isothermal holding within 1040–1120°C for 1.5–5 min.

The proposed model can be used to develop scientific foundations and to substantiate technological regimes for obtaining tantalum alloys from mineral and technogenic raw materials.

ACKNOWLEDGMENTS

This work was performed with the use of the equipment of the Ural-M Shared Access Center.

FUNDING

This work was financially supported by the Russian Foundation for Basic Research (project 18-29-24051_mk).

REFERENCES

1. Mackay, D.A.R. and Simandl, G.J., Geology, market and supply chain of niobium and tantalum—a review, *Miner. Deposita*, 2014, vol. 49, no. 8, pp. 1025–1047.
2. Zelikman, A.N., Korshunov, B.G., Elyutin, A.V., and Zakharov, A.M., *Niobii i tantal* (Niobium and Tantalum), Moscow: Metallurgiya, 1990.
3. Wilhelm, H.A., Bergman, R.M., and Schmidt, F.A., Tantalum metal by bomb reduction of Ta_2O_5, *JOM*, 1970, vol. 22, no. 1, pp. 45–49.
4. Wise, M.A. and Cerny, P., The crystal chemistry of the tapiolite series, *Can. Mineral.*, 1996, vol. 34, no. 3, pp. 631–647.
5. Lyakishev, N.P., Pliner, Yu.L., Ignatenko, G.F., and Lappo, S.I., *Alyuminotermiya* (Aluminothermy), Moscow: Metallurgiya, 1978.
6. Muntera, R., Parshin, A., Yamshchikov, L., Plotnikov, V., Gorkunov, V., and Kobere, V., Reduction of tantalum pentoxide with aluminium and calcium: Thermodynamic modelling and scale skilled tests, *Proc. Est. Acad. Sci.*, 2010, vol. 59, no. 3, pp. 243–252.
7. Mostaan, H., Karimzadeh, F., and Abbasi, M.H., Nonisothermal kinetic studies on the formation of Al_2O_3/Nb composite, *Thermochim. Acta*, 2010, vol. 511, pp. 32–36.
8. Mansurova, A.N., Chumarev, V.M., Leont'ev, L.I., Gulyaeva, R.I., and Sel'menskih, N.I., Phase transformation during the interaction of Ta_2O_5 and $MnTa_2O_6$ with aluminum, *Privolzh. Nauchn. Vestn.*, 2013, no. 12-1 (28), pp. 8–14.
9. Mansurova, A.N., Chumarev, V.M., Leont'ev, L.I., Gulyaeva, R.I., and Sel'menskikh, N.I., Phase transformations during the interaction of Nb_2O_5 and $FeNb_2O_6$ with aluminum, *Russ. Metall. (Metally)*, 2012, vol. 2012, pp. 929–934.
10. Roine, A., *HSC Chemistry 6.12*, Outotec, Pori, 2006. https://www.outotec.com/HSC
11. Opffermann, J., *NETZSCH Thermokinetics, Version 2006.08.* https://www.therm-soft.com
12. *Powder Diffraction File PDF4+ ICDD*, 2019.
13. *DIFFRAC. EVA V5 Bruker AXS*, 2010–2018.
14. Laugier, J. and Checkcell, B.B., *LMGP-Suite of Programs for the Interpretation of X-Ray Experiments*, Saint Martin d'Heres, France: ENSP Lab. Matér. Gén. Phys., 2004. https://www.ccp14.ac.in/tutorial/lmgp/
15. Rietveld, H.M., Line profiles of neutron powder-diffraction peaks for structure refinement, *Acta Crystallogr.*, 1967, vol. 22, pp. 151–152.
16. *DIFFRACPlus: TOPAS Bruker AXS GmbH*, Ostliche, Karlsruhe, Germany, 2008.
17. Gulyaeva, R.I., Petrova, S.A., Chumarev, V.M., and Mansurova, A.N., High-temperature heat capacity and thermal extension of $FeTa_2O_6$, *Phys. Solid State*, 2019, vol. 61, no. 10, pp. 1947–1954.
18. Mansurova, A.N., Chumarev, V.M., and Gulyaeva, R.I., Thermodynamic properties of $FeNb_2O_6$ and $FeTa_2O_6$, *Inorg. Mater.*, 2018, vol. 54, pp. 700–705.
19. Zabeivorota, N.S., Lykasov, A.A., and Mikhailov, G.G., Free energy of the $FeTa_2O_6$ formation reaction at 1470–1750 K, *Izv. Akad. Nauk SSSR, Neorg. Mater.*, 1981, vol. 17, no. 9, pp. 1725–1726.
20. Garg, S.P., Krishnamurthy, N., Awasthi, A., and Venkatraman, M., The O–Ta (oxygen–tantalum) system, *J. Phase Equilib.*, 1996, vol. 17, no. 1, pp. 63–77.
21. Kubaschewski, O. and Alcock, C.B., *Metallurgical Thermochemistry*, Oxford: Pergamon, 1979.
22. Vyazovkin, S., Burnham, A.K., Criado, J.M., Perez-Maqueda, L.A., Popescu, C., and Sbirrazzuoli, N., ICTAC kinetics committee recommendations for performing kinetic computations on thermal analysis data, *Thermochim. Acta*, 2011, vol. 520, pp. 1–19.
23. Vyazovkin, S., Burnham, A.K., Favergeon, L., Koga, N., Moukhina, E., Perez-Maqueda, L.A., and Sbirrazzuoli, N., ICTAC kinetics committee recommendations for analysis of multi-step kinetics, *Thermochim. Acta*, 2020, vol. 689, art. ID 178597.
24. Arshad, M.A. and Maaroufi, A.K., Recent advances in kinetics and mechanisms of condensed phase processes: A mini-review, *Rev. Adv. Mater. Sci.*, 2017, vol. 51, pp. 177–187.
25. Ozawa, T., A new method of analyzing thermogravimetric data, *Bull. Chem. Soc. Jpn.*, 1965, vol. 38, no. 11, pp. 1881–1886.
26. Ozawa, T., Kinetic analysis of derivative curves in thermal analysis, *J. Therm. Anal. Calorim.*, 1970, vol. 2, no. 3, pp. 301–324.
27. Flynn, J.H. and Wall, L.A., General treatment of the thermogravimetry of polymers, *J. Res. Natl. Bur. Stand., Sect. A*, 1966, vol. 70, pp. 487–523.
28. Moukhina, E., Determination of kinetic mechanisms for reactions measured with thermoanalytical instruments, *J. Therm. Anal. Calorim.*, 2012, vol. 109, pp. 1203–1214.
29. Witusiewicz, V.T., Bondar, A.A., Hecht, U., Voblikov, V.M., Tsyganenko, N.I., Fomichov, O.S., Karpets, M.V., Petyukh, V.M., and Velikanova, T.Y., Experimental study and thermodynamic modelling of the ternary Al–Fe–Ta system, *J. Mater. Sci.*, 2013, vol. 48, pp. 377–412.
30. Kitayama, K., Experimental study of equilibria of the Ta_2O_5–Fe–Fe_2O_3 system at 1200°C, *J. Solid State Chem.*, 1986, vol. 64, no. 2, pp. 162–168.
31. Lee, M., Koch, E.F., and Hale, T.E., A study of the coating substrate interface layer of an Al_2O_3-coated cemented carbide cutting tool, *Int. J. Refract. Met. Hard Mater.*, 1996, vol. 14, pp. 335–343.

Translated by A. Tulyabaev